Lithium–Sulfur Batteries Hot Paper

International Edition: DOI: 10.1002/anie.201511632
German Edition: DOI: 10.1002/ange.201511632

Double-Shelled Nanocages with Cobalt Hydroxide Inner Shell and Layered Double Hydroxides Outer Shell as High-Efficiency Polysulfide Mediator for Lithium–Sulfur Batteries

Jintao Zhang, Han Hu, Zhen Li, and Xiong Wen (David) Lou**

Abstract: *Lithium–sulfur (Li-S) batteries have been considered as a promising candidate for next-generation electrochemical energy-storage technologies because of their overwhelming advantages in energy density. Suppression of the polysulfide dissolution while maintaining a high sulfur utilization is the main challenge for Li–S batteries. Here, we have designed and synthesized double-shelled nanocages with two shells of cobalt hydroxide and layered double hydroxides (CH@LDH) as a conceptually new sulfur host for Li–S batteries. Specifically, the hollow CH@LDH polyhedra with complex shell structures not only maximize the advantages of hollow nanostructures for encapsulating a high content of sulfur (75 wt %), but also provide sufficient self-functionalized surfaces for chemically bonding with polysulfides to suppress their outward dissolution. When evaluated as cathode material for Li–S batteries, the CH@LDH/S composite shows a significantly improved electrochemical performance.*

After two decades of optimization, the current Li-ion batteries (LIBs) based on intercalation reactions have approached their energy density limit and will be unable to meet the demands of fast-developing electrical vehicles, large-scale energy storage devices, and advanced portable electronics.[1] Because of the overwhelming advantages in energy density, lithium–sulfur (Li-S) batteries have been considered as a promising candidate for next-generation electrochemical energy-storage technologies.[1,2] In addition, some valuable characteristics of sulfur, such as the high natural abundance, its low costs, and nontoxicity, make Li–S batteries even more commercially competitive than the current LIBs.[3] However, practical applications of the rechargeable Li–S battery are still hindered by a multitude of issues, including low utilization of the active material, short cycle life, fast self-discharge, and poor Coulombic efficiency.[4] The insulating nature of both sulfur and its end products of discharge (Li_2S/Li_2S_2), as well as the dissolution of intermediate polysulfides generated during cycling are the two primary reasons for the poor performance of Li–S batteries. To face these challenges, extensive research efforts have been exerted on cathodes,[5–7] electrolytes,[8–10] separators,[11–13] and lithium-metal anodes[14,15] for preventing the migration of polysulfides and enhancing the use of sulfur. Among these approaches, composing sulfur with conductive carbon frameworks has been proven promising.[16–18] In the pioneering work by Nazar's research group, sulfur is confined within highly ordered mesoporous carbon (CMK-3) and exhibits a reversible capacity over 1000 $mAh\,g^{-1}$ for 20 cycles.[19] Encouraged by this observation, various carbon materials have been further investigated thoroughly for improving the performance of Li–S batteries, including porous carbon,[20–22] carbon nanotubes/fibers,[23–26] graphene,[27,28] hollow carbon structures,[29,30] and combined carbon structures.[31,32] Great progress in both the electrochemical properties and the reaction mechanisms have been achieved.

Although these carbon/sulfur composite cathodes exhibit high specific capacities during the initial cycles, they usually decay rapidly in the subsequent cycles, and the cycling stability remains a significant challenge for practical applications. This problem is often attributed to the dissolution of the reaction intermediate polysulfides in the organic electrolyte. In fact, the weak physical adsorptions provided by the nonpolar carbon substrates could not efficiently suppress the dissolution of polar natured polysulfides during the whole charge–discharge cycling process.[33] In contrast, it has been discovered that some metal oxides/sulfides with polar surfaces can form strong chemical bonds with the lithium polysulfide species. Introducing inorganic anchoring materials as sulfur hosts, such as Ti_4O_7,[33,34] MnO_2,[35,36] and TiS_2,[37] has been demonstrated as an effective way to slow down polysulfide dissolution and therefore achieve long-term cycling stability. However, considering the high volume ratio of sulfur and the metal oxides/sulfides, it is often a concern that the anchoring powder, even with nanoscale particle sizes, would not be able to provide sufficient interfaces to fix all polysulfide species in the electrode. A more practical way is to apply the limited anchoring materials as the coating layers. More recently, thin-layered metal hydroxides, including $Co(OH)_2$[38] and $Ni_3(NO_3)_2(OH)_4$,[39] have been used as effective encapsulation materials for the sulfur cathodes. In one case, Yu's research group demonstrated that $Ni_3(NO_3)_2(OH)_4$ could turn into layered (Li,Ni)-mixed hydroxide compounds by irreversibly reacting with Li^+ ions during the early cycles.[39] This result suggests the possibility of using layered transition-metal hydroxides as promising encapsulation materials to build better Li–S cells. Unfortunately, restricted by the undesired polarizations of the electrode and the inevitable process of the slow transformation from $Ni_3(NO_3)_2(OH)_4$ to layered (Li,Ni)-mixed hydroxides, this hybrid cathode material is still far

[*] J. Zhang, Dr. H. Hu, Dr. Z. Li, Prof. X. W. Lou
School of Chemical and Biomedical Engineering
Nanyang Technological University
62 Nanyang Drive, Singapore 637459 (Singapore)
E-mail: li_zhen@ntu.edu.sg
xwlou@ntu.edu.sg
Homepage: http://www.ntu.edu.sg/home/xwlou/

Supporting information for this article can be found under http://dx.doi.org/10.1002/anie.201511632.

away from real-world production and application.[39] As a consequence, there is still an urgent need to explore new materials as sulfur hosts for the practical use of Li–S batteries.

Layered double hydroxides (LDHs) are a class of anionic clays with 2D structures, which have been widely used for catalysis as catalyst precursors, bioactive nanocomposites, electroactive and photoactive materials.[40] The general formula of LDHs is $[M^{2+}_{1-x}M^{3+}_{x}(OH)_2]\ [A^{n-}_{x/n}]\cdot m\,H_2O$, where M^{2+} is a divalent cation and M^{3+} a trivalent cation, while A^{n-} is a charge-balancing interlayer anion.[40] Benefitting from the abundant hydrophilic and hydroxy groups, LDHs might be an ideal polysulfide mediator based on previous findings.[38,39,41] In addition, the electrocatalysis of LDHs may also enhance the reaction kinetics of lithium polysulfides redox reactions,[40,42] and the high anion exchange capability may entrap polysulfide anions within the interlayers,[43,44] effectively suppressing the dissolution of polysulfides into the organic electrolyte. To the best of our knowledge, rare investigations have been reported on using LDHs as sulfur hosts for Li–S batteries.

Herein, we have designed and synthesized a novel type of double-shelled $Co(OH)_2$/LDH (noted as CH@LDH) nanocages as a new sulfur host for Li–S batteries. The concept of the CH@LDH/S composite cathode has multiple advantages. Specifically, the outer LDH and inner $Co(OH)_2$ hollow polyhedra with complex shell structures not only maximize the advantages of hollow nanostructures for encapsulating a large amount of sulfur,[29] but also provide a relatively large functional surface for chemically bonding with polysulfides to suppress their outward dissolution. When evaluated as the cathode material for Li–S batteries, the CH@LDH/S composite shows significantly improved electrochemical performances.

The synthesis process of double-shelled CH@LDH nanocages and CH@LDH/S is shown in Figure 1 (for experimental details see the Supporting Information). First, a rhombic dodecahedral ZIF-67 particle is fabricated as a sacrificial template. Then, hollow polyhedral LDH shells are formed on ZIF-67 (denoted as ZIF-67@LDH) by reacting with $Ni(NO_3)_2$ in ethanol. Following that, double-shelled CH@LDH nanocages are fabricated by reacting the single-shelled ZIF-67@LDH with an aqueous solution of Na_2MoO_4. Finally, sulfur is loaded into double-shelled CH@LDH nanocages by a melting-diffusion method.

ZIF-67 particles are fabricated as previously reported.[45] As shown in the field-emission scanning electron microscopy (FESEM) and transmission electron microscopy (TEM) images (Figure 2a,e), the as-prepared ZIF-67 particles have the uniform shape of a rhombic dodecahedron with a smooth surface, and an average particle size of about 800 nm with a narrow size distribution (see Figure S1 in the Supporting Information). The X-ray diffraction (XRD) pattern of ZIF-67 matches well with the simulated pattern (Figure S2a), and the energy-dispersive X-ray (EDX) spectroscopy result confirms the chemical composition of the crystals (Figure S2b), demonstrating the high purity of the material phase. By using ZIF-67 as the sacrificial template and reacting with $Ni(NO_3)_2$ in ethanol solution for 30 minutes, the Ni–Co LDH polyhedral nanoshells are successfully formed in the same morphology and dimension of ZIF-67 (Figure 2b).[45] The rougher surface assembled by small nanosheets indicates the thin layer-shaped LDH morphology. The chemical formula of the LDH shell might be expressed as $[Ni^{2+}_{1/3}Co^{3+}_{2/3}(OH)_2][NO_3^{2-}{}_{1/3}]\cdot mH_2O$ based on the molar Ni/Co ratio of about 1:2 (Figure S3). The yolk–shell structure of the sample can be revealed by TEM (Figure 2f)and shows a well-developed inner cavity. The core with a smooth surface has a similar polyhedral shape as the original ZIF-67, while the shell is composed of interconnected small nanosheets. The XRD pattern shows that the crystal phase of the single-shelled product is still mainly composed of ZIF-67 (Figure S2c), which is further supported by the EDX result showing a similar elemental composition as ZIF-67 (Figure S2d). After the reaction with aqueous solution of Na_2MoO_4, the product well inherits the morphology and dimensions of the integrated nanosheet-assembled shells (Figure 2c). The inner ZIF-67 yolk is transformed into a hollow structured nanocage, forming novel double-shell structured nanocages (Figure 2g). The double-shelled nanocages have a specific surface area of 117 $m^2 g^{-1}$ (Figure S4), which could provide sufficient surface for chemically bonding with polysulfides. After sulfur is loaded into the double-shelled CN@LDH nanocages, the CH@LDH/S composite particles maintain the polyhedral shape (Figure 2d). The darker contrast of the inside region of the CH@LDH/S composite indicates the diffusion of sulfur into the inner space (Figure 2h), revealing that sulfur has been homogeneously encapsulated within the LDH shells.

Figure 3a shows the XRD result of the as-prepared double-shelled CH@LDH nanocages. After the reaction of ZIF-67@LDH with water solution of Na_2MoO_4, the diffraction peaks of ZIF-67 totally disappear, and the diffraction peak at 18.9° corresponds relatively well to $Co(OH)_2$.[38] MoO_4^{2-} anions are not directly involved in the chemical

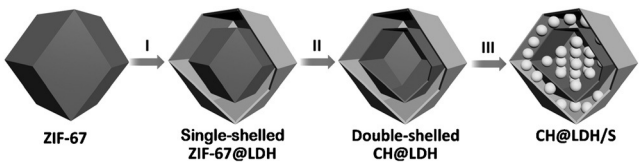

Figure 1. Schematic illustration of the synthesis of the CH@LDH/S composite.

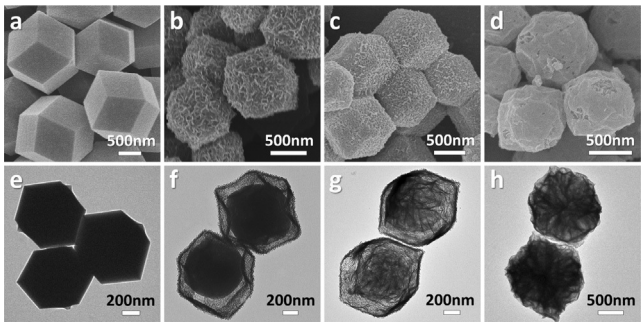

Figure 2. SEM and TEM images of a,e) ZIF-67, b,f) single-shelled ZIF-67@LDH, c,g) double-shelled CH@LDH nanocages, and d,h) CH@LDH/S.

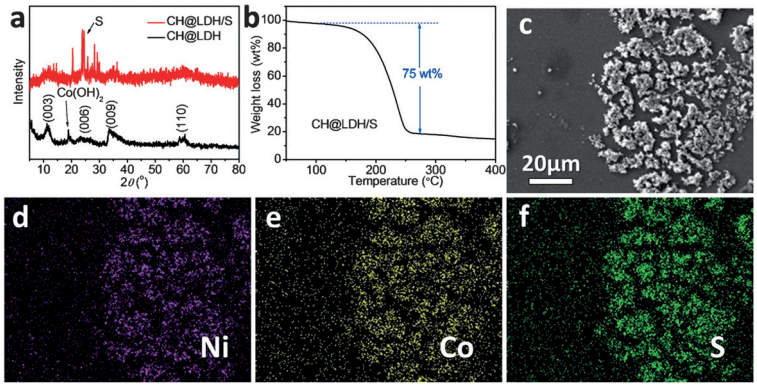

Figure 3. a) XRD patterns of the double-shelled CH@LDH nanocages and the CH@LDH/S composite. b) TGA curve of CH@LDH/S in N_2 atmosphere with a heating rate of 10 °C min^{-1}. c) SEM image of CH@LDH/S and corresponding EDX elemental mappings of d) Ni, e) Co and f) S.

reaction with the inner ZIF-67; instead the OH^- ions generated by hydrolysis of MoO_4^{2-} anions precipitate with Co^{2+} ions released from ZIF-67 to form $Co(OH)_2$. On the other hand, the distinguishable (003), (006), (009), and (110) peaks of the product can be clearly ascribed to a typical Ni–Co LDH structure.[45] After loaded with sulfur, the diffraction peaks of $Co(OH)_2$ and LDH become relatively weak, all strong diffraction peaks come from the crystalline sulfur in the CH@LDH/S composite (Figure 3a). The mass loading of sulfur in the CH@LDH/S composite is determined by thermogravimetric analysis (TGA) to be as high as 75 wt% (Figure 3b), which may promise both high volumetric and gravimetric energy densities of the electrode material for Li–S batteries.[46] The EDX spectrum of the CH@LDH nanocages indicates that Ni and Co are the two major metal elements in the double-shelled framework with a small amount (<5 wt%) of Mo incorporated (Figure S5). The strong EDX signal of sulfur in the CH@LDH/S composite indicates the large amount of sulfur in the final cathode electrode material (Figure S5). The distribution of different elements in the CH@LDH/S composite is investigated by EDX mapping analysis under SEM observation (Figure 3c–f). The uniform distributions of Co and Ni elements suggest that the double-shelled CH@LDH structures are formed in almost all particles. The signal of sulfur is uniformly matched with the CH@LDH region, indicating the good confinement of sulfur within the CH@LDH frameworks.

To evaluate the electrochemical cycling performance of the CH@LDH/S composite, 2032-type coin cells are fabricated with thick coated electrode films (Figure S6), in which the areal mass loading of sulfur is controlled to be approximately 3 mg cm^{-2}. To show the effects of CH@LDH on retarding polysulfide dissolution, a mesoporous carbon/sulfur composite (denoted as C/S) is also measured by the same conditions for comparison. As shown in Figure 4a, the CH@LDH/S composite delivers an initial discharge capacity of 1014 mAh g^{-1} at 0.1 C, which is very close to the initial discharge capacity of 1068 mAh g^{-1} achieved by the C/S composite, revealing that the CH@LDH host would not obviously increase the polarization of the cells in the early stage of cycling. Different from the Ni-based hydroxide ($Ni_3(NO_3)_2(OH)_4$), which gradually transformed into (Ni,Li)-mixed hydroxides during dozens of charge–discharge cycles,[39] the CH@LDH framework shows stable electrochemical properties at the beginning of the electrochemical tests. The stable cyclic voltammetry (CV) curves of a pure CH@LDH electrode further confirm its electrochemical stability (Figure S7). Moreover, based on recently reported electrocatalysis principles to the Li–S batteries,[42,47] the CH@LDH host may also enhance the reaction kinetics of the sulfur cathode because of its inherent catalytic properties.[40] In the following cycles, the C/S composite shows a reversible capacity of 450 mAh g^{-1} after only 60 cycles. In contrast, the CH@LDH/S composite maintains

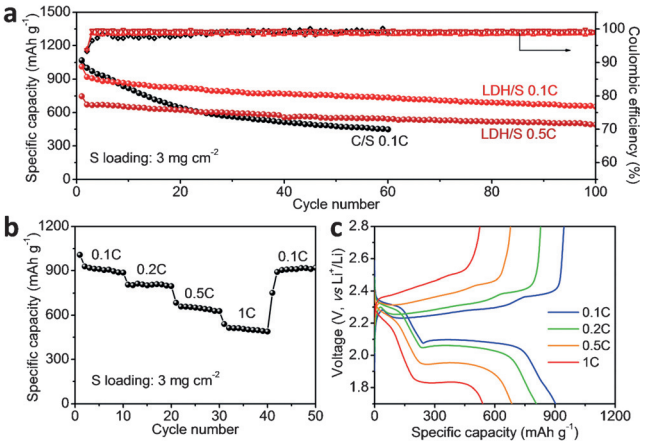

Figure 4. a) Cycle performance comparison between CH@LDH/S and C/S. b) Discharge capacities and c) voltage profiles of CH@LDH/S at various current densities from 0.1 to 1 C.

much better capacity retention of 736 mAh g^{-1} after the same number of cycles, and still delivers a reversible capacity of 653 mAh g^{-1} at the 100th cycle, indicating that the CH@LDH host successfully suppresses the outward diffusion of soluble polysulfides. A visual observation of solution-phase polysulfide adsorption further demonstrates that CH@LDH has much better capability of adsorbing lithium polysulfides than the carbon materials (Figure S8). When cycled in the electrolyte without $LiNO_3$ additive, the C/S composite shows an obvious overcharge (Figure S9a), indicating significant dissolution of polysulfides; while the CH@LDH/S composite still exhibits a high Coulombic efficiency (Figure S9b), further revealing that the CH@LDH host can effectively restrict the dissolution of polysulfides. When cycled at 0.5 C, the CH@LDH/S composite also exhibits stable cycle life, over which the discharge capacity slowly decreases from initially 747 mAh g^{-1} to 491 mAh g^{-1} by the 100th cycle. Considering the relatively high areal mass loading of sulfur, the cycling performance is competitive to previously reported work.

To evaluate the rate capability of CH@LDH/S, cells with sulfur mass loading of 3 mg cm^{-2} are cycled at various current densities for 0.1 to 1 C (Figure 4b). The discharge capacity of CH@LDH/S is stabilized at >900 mAh g^{-1} at 0.1 C, corresponding to an areal capacity of 2.7 mAh cm^{-2}. Further cycling at 0.2, 0.5, and 1 C shows high reversible capacities of 800, 650 and 500 mAh g^{-1}, respectively (Figure 4b and c), indicating excellent reaction kinetics of the CH@LDH/S electrode. When the current density is reduced back to 0.1 C, a reversible capacity of 904 mAh g^{-1} is achieved, indicating a good stability of the electrode material after high current density tests. The excellent electrochemical performance is attributed to the multiple advantages of this novel cathode structure. First, the hollow structure provides sufficient void space for loading a large amount of active materials. Second, the hydroxy-functionalized polar surfaces have strong binding affinities toward lithium polysulfides, which can efficiently suppress the dissolution of polysulfides and thus keep good cycling stability. Third, the CH@LDH host can enhance the reaction kinetics of the sulfur electrode, giving rise to high rate properties even with high areal mass loading of sulfur.

In summary, we have demonstrated a new concept of using double-shelled CH@LDH nanocages as a sulfur host for Li–S batteries. With this novel design, the CH@LDH/S composite is loaded with a high content of sulfur (75 wt%), and the Li–S battery with the CH@LDH/S cathode is able to maintain excellent cycling stability at both 0.1 and 0.5 C over 100 cycles, and deliver high-rate capacities with relatively high sulfur loading of 3 mg cm^{-2}. The concept of introducing layered double hydroxides in the Li–S battery system will open a new avenue for future development of high performance Li–S batteries.

Acknowledgements

X.W.L. is grateful to the Ministry of Education (Singapore) for financial support through the AcRF Tier 1 funding (Grant RG12/14; grant number M4011258).

Keywords: electrochemical performance · double-shelled nanocages · layered double hydroxides · lithium–sulfur batteries · nanostructures

How to cite: *Angew. Chem. Int. Ed.* **2016**, *55*, 3982–3986
Angew. Chem. **2016**, *128*, 4050–4054

[1] P. G. Bruce, S. A. Freunberger, L. J. Hardwick, J. M. Tarascon, *Nat. Mater.* **2012**, *11*, 19–29.
[2] X. L. Ji, L. F. Nazar, *J. Mater. Chem.* **2010**, *20*, 9821–9826.
[3] A. Manthiram, Y. Fu, S. H. Chung, C. Zu, Y. S. Su, *Chem. Rev.* **2014**, *114*, 11751–11787.
[4] S. Evers, L. F. Nazar, *Acc. Chem. Res.* **2013**, *46*, 1135–1143.
[5] Y. Yang, G. Zheng, Y. Cui, *Chem. Soc. Rev.* **2013**, *42*, 3018–3032.
[6] L. Ma, K. E. Hendrickson, S. Wei, L. A. Archer, *Nano Today* **2015**, *10*, 315–338.
[7] L. Ma, H. L. Zhuang, Y. Y. Lu, S. S. Moganty, R. G. Hennig, L. A. Archer, *Adv. Energy Mater.* **2014**, *4*, 1400390.
[8] S. S. Zhang, *J. Power Sources* **2013**, *231*, 153–162.
[9] Z. Lin, Z. Liu, W. Fu, N. J. Dudney, C. Liang, *Angew. Chem. Int. Ed.* **2013**, *52*, 7460–7463; *Angew. Chem.* **2013**, *125*, 7608–7611.
[10] L. Suo, Y. S. Hu, H. Li, M. Armand, L. Chen, *Nat. Commun.* **2013**, *4*, 1481.
[11] G. Zhou, L. Li, D. W. Wang, X. Y. Shan, S. Pei, F. Li, H. M. Cheng, *Adv. Mater.* **2015**, *27*, 641–647.
[12] H. B. Yao, K. Yan, W. Y. Li, G. Y. Zheng, D. S. Kong, Z. W. Seh, V. K. Narasimhan, Z. Liang, Y. Cui, *Energy Environ. Sci.* **2014**, *7*, 3381–3390.
[13] J. Q. Huang, Q. Zhang, H. J. Peng, X. Y. Liu, W. Z. Qian, F. Wei, *Energy Environ. Sci.* **2014**, *7*, 347–353.
[14] C. Huang, J. Xiao, Y. Shao, J. Zheng, W. D. Bennett, D. Lu, S. V. Laxmikant, M. Engelhard, L. Ji, J. Zhang, X. Li, G. L. Graff, J. Liu, *Nat. Commun.* **2014**, *5*, 3015.
[15] G. Ma, Z. Wen, M. Wu, C. Shen, Q. Wang, J. Jin, X. Wu, *Chem. Commun.* **2014**, *50*, 14209–14212.
[16] Z. Li, Y. Huang, L. Yuan, Z. Hao, Y. Huang, *Carbon* **2015**, *92*, 41–63.
[17] X. Fang, H. Peng, *Small* **2015**, *11*, 1488–1511.
[18] J. G. Wang, K. Xie, B. Wei, *Nano Energy* **2015**, *15*, 413–444.
[19] X. L. Ji, K. T. Lee, L. F. Nazar, *Nat. Mater.* **2009**, *8*, 500–506.
[20] H. B. Wu, S. Wei, L. Zhang, R. Xu, H. H. Hng, X. W. Lou, *Chem. Eur. J.* **2013**, *19*, 10804–10808.
[21] Z. Li, L. X. Yuan, Z. Q. Yi, Y. M. Sun, Y. Liu, Y. Jiang, Y. Shen, Y. Xin, Z. L. Zhang, Y. H. Huang, *Adv. Energy Mater.* **2014**, *4*, 1301473.
[22] Z. Li, Y. Jiang, L. Yuan, Z. Yi, C. Wu, Y. Liu, P. Strasser, Y. Huang, *ACS Nano* **2014**, *8*, 9295–9303.
[23] J. C. Guo, Y. H. Xu, C. S. Wang, *Nano Lett.* **2011**, *11*, 4288–4294.
[24] H. Yao, G. Zheng, W. Li, M. T. McDowell, Z. Seh, N. Liu, Z. Lu, Y. Cui, *Nano Lett.* **2013**, *13*, 3385–3390.
[25] Z. Li, J. T. Zhang, Y. M. Chen, J. Li, X. W. Lou, *Nat. Commun.* **2015**, *6*, 8850.
[26] L. Ma, H. L. Zhuang, S. Wei, K. E. Hendrickson, M. S. Kim, G. Cohn, R. G. Hennig, L. A. Archer, *ACS Nano* **2015**, *10*, 1050–1059.
[27] Z. Wang, Y. Dong, H. Li, Z. Zhao, H. Wu, C. Hao, S. Liu, J. Qiu, X. W. Lou, *Nat. Commun.* **2014**, *5*, 5002.
[28] G. Zhou, E. Paek, G. S. Hwang, A. Manthiram, *Nat. Commun.* **2015**, *6*, 7760.
[29] C. Zhang, H. B. Wu, C. Yuan, Z. Guo, X. W. Lou, *Angew. Chem. Int. Ed.* **2012**, *51*, 9592–9595; *Angew. Chem.* **2012**, *124*, 9730–9733.
[30] N. Jayaprakash, J. Shen, S. S. Moganty, A. Corona, L. A. Archer, *Angew. Chem. Int. Ed.* **2011**, *50*, 5904–5908; *Angew. Chem.* **2011**, *123*, 6026–6030.
[31] M. Q. Zhao, X. F. Liu, Q. Zhang, G. L. Tian, J. Q. Huang, W. Zhu, F. Wei, *ACS Nano* **2012**, *6*, 10759–10769.
[32] C. Tang, Q. Zhang, M. Q. Zhao, J. Q. Huang, X. B. Cheng, G. L. Tian, H. J. Peng, F. Wei, *Adv. Mater.* **2014**, *26*, 6100–6105.
[33] Q. Pang, D. Kundu, M. Cuisinier, L. F. Nazar, *Nat. Commun.* **2014**, *5*, 4759.
[34] X. Tao, J. Wang, Z. Ying, Q. Cai, G. Zheng, Y. Gan, H. Huang, Y. Xia, C. Liang, W. Zhang, Y. Cui, *Nano Lett.* **2014**, *14*, 5288–5294.
[35] X. Liang, C. Hart, Q. Pang, A. Garsuch, T. Weiss, L. F. Nazar, *Nat. Commun.* **2015**, *6*, 5682.
[36] Z. Li, J. Zhang, X. W. Lou, *Angew. Chem. Int. Ed.* **2015**, *54*, 12886–12890; *Angew. Chem.* **2015**, *127*, 13078–13082.
[37] Z. W. Seh, J. H. Yu, W. Li, P. C. Hsu, H. Wang, Y. Sun, H. Yao, Q. Zhang, Y. Cui, *Nat. Commun.* **2014**, *5*, 5017.
[38] X. Niu, X. Wang, D. Wang, Y. Li, Y. Zhang, Y. Zhang, T. Yang, T. Yu, J. Tu, *J. Mater. Chem. A* **2015**, *3*, 17106–17112.
[39] J. Jiang, J. Zhu, W. Ai, X. Wang, Y. Wang, C. Zou, W. Huang, T. Yu, *Nat. Commun.* **2015**, *6*, 8622.
[40] Q. Wang, D. O'Hare, *Chem. Rev.* **2012**, *112*, 4124–4155.
[41] C. Zu, A. Manthiram, *Adv. Energy Mater.* **2013**, *3*, 1008–1012.
[42] H. Al Salem, G. Babu, C. V. Rao, L. M. Arava, *J. Am. Chem. Soc.* **2015**, *137*, 11542–11545.

[43] S. Ma, Y. Shim, S. M. Islam, K. S. Subrahmanyam, P. Wang, H. Li, S. Wang, X. Yang, M. G. Kanatzidis, *Chem. Mater.* **2014**, *26*, 5004 – 5011.
[44] S. Ma, L. Huang, L. Ma, Y. Shim, S. M. Islam, P. Wang, L. D. Zhao, S. Wang, G. Sun, X. Yang, M. G. Kanatzidis, *J. Am. Chem. Soc.* **2015**, *137*, 3670 – 3677.
[45] H. Hu, B. Guan, B. Xia, X. W. Lou, *J. Am. Chem. Soc.* **2015**, *137*, 5590 – 5595.
[46] J. Gao, H. D. Abruña, *J. Phys. Chem. Lett.* **2014**, *5*, 882 – 885.
[47] G. Babu, K. Ababtain, K. Y. Ng, L. M. Arava, *Sci. Rep.* **2015**, *5*, 8763.

Received: December 15, 2015
Published online: February 19, 2016

